

Predicting the behavior of geogrid while used as reinforcement in a slope fill under footing load



Md. Ariful Islam & C. T. Gnanendran
School of Engineering and Information Technology
University of New South Wales @ Australian Defence Force Academy
Canberra, ACT - 2600, Australia.

ABSTRACT

The numerical analysis results of the stabilizing force provided by a geogrid reinforcement layer embedded in the body of a sloped fill subjected to footing load near the crest is summarized in this paper. The foundation soil was modeled by strain softening model with non-linear stiffness behavior using Duncan and Chang's equation. Finite difference computer program, FLAC3D was used to create the geogrid reinforcement and extract the tensile force developed at different locations while footing load was applied. These numerical analysis results were compared with published experimental results and reported in this paper.

RÉSUMÉ

Les résultats d'analyse numérique de la force de stabilisation fournis par une couche de renfort géogrid incorporé dans le corps d'un résumé en pente remplir soumis à une charge pied près de la crête est dans le présent document. Le sol de fondation a été modélisée par adoucissement modèle avec rigidité des comportements non linéaires à l'aide Duncan et l'équation de Chang. programme informatique à différences finies, FLAC3D a été utilisé pour créer le renforcement géogrid et d'extraire la force de traction développée à différents endroits en charge de pied a été appliquée. Ces résultats d'analyse numérique ont été comparés avec les résultats expérimentaux publiés et présentés dans le présent document.

1 INTRODUCTION

Foundation, which is the most important part of any structure, is designed based on soil condition at the construction site. If the foundation soil is weak, deep foundations are generally recommended, which increases both the cost and time of construction. In order to ensure economy, shallow foundations with single or multi layers of reinforcement below it are used now a days, and is the focus of this investigation.

In many situations foundation needs to be constructed on or near slopes e.g. foundation of bridge abutment. The design of foundation on slope need to consider mechanical stability of slope as it affects both bearing capacity and settlement behavior. Geosynthetic reinforcement increases the bearing capacity of sloped fill and improves the settlement behavior of foundation on it. Although geogrids are superior form of reinforcement than geotextile due to soil particle interlocking with the grid aperture, which is particularly true for coarser soil (e.g. gavel) than fine soil (fine sand, clay) (Guido *et al.*, 1986).

The study on the effect of geogrid reinforcement on foundation behavior near the crest of slope has been done by many researchers (Selvadurai and Gnanendran, 1989; Yoo, 2001; Alamshahi and Hataf, 2009). All of them concluded that the inclusion of geogrid reinforcement in foundation soil enhance load carrying capacity and improve load-settlement behavior of foundation near slope, if geogrid is placed at optimum

layout. Based on physical model study, some of them tried to estimate the tensile force and strain developed in geogrid when used as reinforcement in foundation soil slope (Gnanendran and Selvadurai, 2001; Bathurst *et al.*, 2003). Because the knowledge of the bearing capacity of reinforced soil or settlement behavior of foundation supported on it and tensile force or strain developed in the geogrid are required for efficient engineering design of such structure.

Selvadurai and Gnanendran (1989) conducted small scale physical model study on footing located near the crest of single layer geogrid reinforced slope fill and concluded that the optimum location of geogrid reinforcement occurs at a depth between 0.5 and 0.9 times the width of foundation. Based on their experimental data on bearing capacity and settlement behavior improvement of foundation on slope fill structure with different position of geogrid reinforcement, Thanapalasingam and Gnanendran, (2008) developed a 3D numerical model. Gnanendran and Selvadurai (2001) also published experimental data on tensile force or strain developed in the geogrid used as reinforcement in a slope fill while vertical monotonic load is applied on the footing. But measuring the strain and stabilizing force developed in the geogrid reinforcement while vertical monotonic load is applied on the footing through finite element analysis is very difficult. Using numerical analysis software AFENA, Gnanendran (2001) tried to model the stabilizing force developed in the geogrid reinforcement, but he fails to get a satisfactory

prediction. In this paper numerical analysis software FLAC3D is used to create 3D model slope and geogrid reinforcement in order to model stabilizing force developed in the geogrid reinforcement while vertical load is applied on footing.

2 SCOPE OF THIS ANALYSIS

Although it is possible to determine the tensile force developed in the geogrid reinforcement at different location for a small scale physical model test problem (though it is a tedious job), but in practical cases where large dimension geogrids are used for reinforcing huge soil mass, determination of the tensile force by measuring strain become unrealistic. Thus the numerical analysis result can be a good option to obtain such data if it is first calibrated with the available small scale experimental data.

3 BRIEF DESCRIPTION OF SELECTED PROBLEM

The small scale physical model study on “strain measurement and interpretation of stabilizing force in geogrid reinforcement” by Gnanendran and Selvadurai (2001) was selected for the numerical analysis as experimental data required for calibrating the numerical model were available. In this experimental study the load settlement behavior of a footing located near the crest of reinforced slope and the progressive development of stabilizing force in the geogrid was investigated. (See Selvadurai and Gnanendran, 1989; and Gnanendran and Selvadurai, 2001 for further details). Details of the laboratory experimental setup are shown in figure 1. Model slope was constructed by compacting mortar sand with 5% water content in a reinforced concrete tank of dimensions 1500mm * 880mm * 1200mm depth. After reaching desired elevation geogrid reinforcement was placed and finally compacted fill was excavated to form slope of 1V:2H. Vertical load was applied at a rate of 0.02 mm/sec through a strip footing of dimension 870mm * 104mm in plan area. Load cell and LVDTs were used to measure applied load and related displacement of the footing. The polypropylene biaxial Tensar BX1200 (SS2) geogrid sample used as reinforcement was instrumented with 12 pairs of (Showa N11-FA-5-120-11) foil strain gauges along the centre line to measure average strain developed in the geogrid while applying footing load. Those strain gauges were calibrated to calculate actual tensile force developed in the geogrid. The geogrid reinforcement was embedded at a depth of 0.75 times width of the footing, which was expected to give maximum improvement in footing bearing capacity, based on studies reported by Selvadurai and Gnanendran (1989).

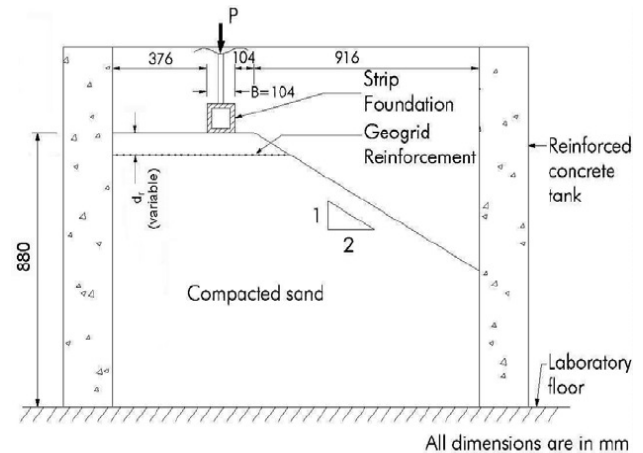


Figure 1: Schematic of the model test facility and layout of instrumentation (after Gnanendran and Selvadurai, 2001)

4 OVERVIEW OF NUMERICAL STUDY

4.1 Details Of Geometry And Boundary Conditions

In order to analyze the footing near reinforced sloped fills and development of progressive stabilizing force in geogrid reinforcement, finite difference computer program FLAC3D was used to develop a 3D numerical model of same geometry and dimensions tested by Gnanendran and Selvadurai (2001). Figure 2 shows 3D view of the generated finite difference mesh where a total of 58000 brick and uniform wedge shaped zones were used to represent the foundation soil of this model. All zones were equally spaced and the dimensions of all zones in the model were kept about 26 mm in all directions so that no lanky shaped zone can affect the numerical calculation. The sides and bottom of the generated finite difference mesh was then fixed in x direction at $x = 0.0$ m and $x = 1.5$ m planes, in y direction at $y = 0.0$ m and $y = 0.88$ m planes and in z directions at $z = 0.0$ m plane

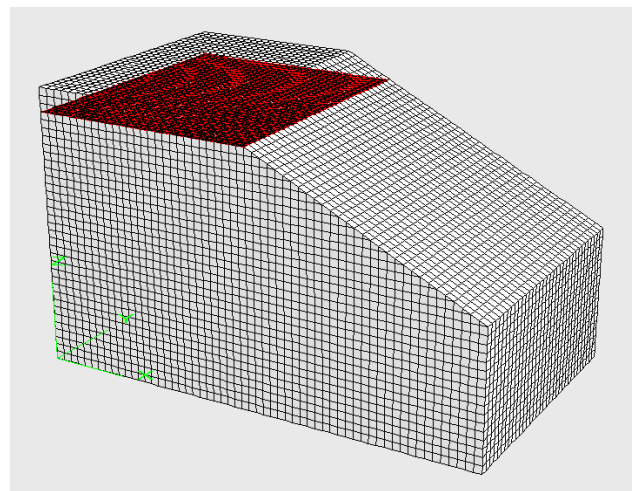


Figure 2: 3D view of the generated finite difference mesh with geogrid reinforcement

4.2 Creating Geogrid Reinforcement

The geogrid reinforcement and geogrid-soil interface were modeled using the built in geogrid structural element given in FLAC3D software which allows to create the geogrid reinforcement as a flat solid membrane rather than grid like structure as shown in figure 2. They are three-noded, flat, finite elements interconnected at edges to form a sheet that can resist tensile force but does not resist bending loading. Jewell *et al.* (1984) identified three main mechanisms of soil - reinforcement interaction of which the soil particle interlocked at grid openings provide additional bearing resistance causing supremacy of geogrid over geotextile. This is particularly true if the particle size of soil where geogrid is embedded is almost same to geogrid apertures size (e.g. gravel). If the soil particle size is very small compared to geogrid apertures size (e.g. fine sand or clay), the bearing action due to particle interlocking became insignificant. As the experimental result published by Gnanendran and Selvadurai (2001) which is analysed here, are obtained by small scale physical model study on geogrid reinforced sand slope. So, by using built-in flat solid membrane like structural element available in the software can be a good option to create geogrid and analyze it.

The geogrid was first created on the bottom surface of the generated finite difference mesh and shifted to desired location. The dimensions of the geogrid sheet were selected such that after shifting to its final position, there is no extra portion out of the soil mesh.

4.3 Selection Of Constitutive Model

The foundation soil was modeled using the strain softening model with non-linear stiffness behavior. It is to be noted that the strain softening model used here is not the actual one. It is based on Mohr-coulomb model. The only difference is that, in strain softening model the strength properties e.g. friction angle, dilation angle, cohesion and tensile strength may harden or soften (as user wants with his desired rate) after the onset of plastic yield whereas in the Mohr-Coulomb model, those properties are assumed to remain constant. There was not enough information regarding how to set the variations of these strength parameters with plastic strain. Therefore, the footing near the crest of reinforced sloped fill model problem with geogrid reinforcement at a depth of 0.75B below the footing was analysed with certain assumed variation of strength parameter with plastic strain to obtain the footing load - settlement plot. The assumed strength parameters with plastic strain were changed until a good load-settlement plot obtained that matched with experimental plot.

It is necessary to consider both the stress dependent stiffness characteristics of soil as well as plastic failure,

to get reasonable stress and strain in the reinforced slope fill. Thus, Duncan's equation was used to model the non linear stiffness characteristic of the foundation soil (Duncan and Chang, 1970). According to this equation, the tangent elastic modulus (E_t) value for any stress condition may be expressed as

$$E_t = \left[1 - \frac{R_f (1 - \sin \phi) (\sigma_1 - \sigma_3)}{2C \cos \phi + 2\sigma_3 \sin \phi} \right]^2 K_e P_a \left(\frac{\sigma_3}{P_a} \right)^n \quad (1)$$

Where,

R_f = failure ratio

σ_1 and σ_3 = major and minor principal stresses respectively

ϕ = angle of internal friction

C = cohesion

P_a = atmospheric pressure

K_e = elastic modulus number

n = elastic exponent for the modulus

Again, the bulk modulus (K) of soil was expressed as

$$K = K_b P_a \left(\frac{\sigma_3}{P_a} \right)^m \quad (2)$$

Where,

K_b = bulk modulus number

m = bulk modulus exponent

The Poisson's ratio (ν) was determined from the calculated bulk modulus by elastic theory as

$$\nu = \frac{1}{2} - \frac{E_t}{6K} \quad (3)$$

The value of ν was set to range between $0 \leq \nu \leq 0.49$ using a subroutine of the program.

4.4 Selection of Material Parameters

The physical properties of materials (sand and geogrid) was set almost similar to that obtained by Gnanendran and Selvadurai, (2001) from their laboratory experiments while studying small scale physical model problem (See Selvadurai and Gnanendran, 1989; and Gnanendran and Selvadurai, 2001 for further details). The material parameters for sand are shown in table 1.

Table 1. Properties of sand.

materials	Properties	values
-----------	------------	--------

sand	Unit weight	17.6 KN/m ³
	Water content	5%
	Friction angle	43°
	Dilation angle	13°
	Cohesion	3 KPa
	Tensile strength	Nil
	Modulus of elasticity	Variable with minimum value 18 MPa
	Poisson's ratio	Varying between 0 & 49

The variation of strength properties with plastic strain to capture the after failure load deformation behavior are shown in table 2

Table 2. Strain softening parameters.

Plastic strain value	Variation of Friction angle	Variation of Dilation angle	Variation of cohesion	Variation of Tensile strength
0%	43°	13°	3 KPa	Nil
1%	47°	17°	3 KPa	Nil
1.3%	44°	13°	3 KPa	Nil
20%	35°	5°	2 KPa	Nil

Duncan's equation parameters were obtained by calibrating the 3D numerical analysis data with the experimental data of footing near reinforced sloped fills. The analytical and experimental footing load-displacement behaviour of the reinforced sloped fill - footing model with strain softening behaviour is shown in Fig 4. A minimum value of 18 MPa for tangent modulus was set to avoid the numerical instability due to lower values of σ_3 at anytime during the numerical simulation. The adopted parameters for Duncan's equation for the current 3D modelling are presented in table 3.

Table 3. Duncan's equation parameters.

Duncan's equation parameters	Values
Failure ratio	0.86
Elastic modulus number, K_e	1150
Elastic modulus exponent, n	0.5
Bulk modulus number, K_b	575
Bulk modulus exponent, m	0.5
Atmospheric pressure, P_a	101.3 KPa

The material constitutive behaviour for the geogrid element was assumed as isotropic. The spring-slider mechanism was used to model soil – geogrid interface,

with three coupling spring properties, which were given to control the shear behaviour of the soil - geogrid interface. The required soil - geogrid interface properties e.g. coupling spring cohesion, coupling spring frictional angle and coupling spring stiffness were obtained by calibrating the reinforced sloped fill - footing model with a single layer of reinforcement layer at 0.75B depth of embedment. The properties of geogrid reinforcement used in this analysis are shown in table 4.

Table 4. Properties of geogrid reinforcement.

materials	Properties	Values
Geogrid	Density	950 kg/m ³
	Thickness	2 mm
	Isotropic elastic modulus	0.8 GPa
	Poisson's ratio	.33
	Coupling spring stiffness	2.3e9 N/m ³
	Coupling spring friction angle	30°
	Coupling spring cohesion	Nil
	Large strain slide	On

5 VALIDATION OF 3D NUMERICAL MODEL

3D numerical model was developed to predict the performance of a footing near reinforced sloped fill with a single layer of reinforcement placed at a particular depth (e.g. 0.75B) from footing base. The predicted performance (load settlement behaviour) from 3D numerical model was compared with the reported performance of the laboratory model test data published by Gnanendran and Selvadurai (2001). A very good match (as shown in the figure 3) between the predicted and measured footing load - displacement behaviour was obtained and thereby 3D numerical models were verified.

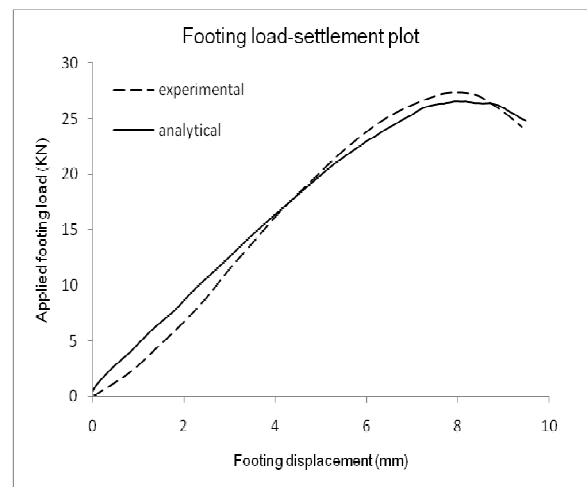


Figure 3: Load-settlement relationship of footing located on reinforced sloped fill

6 RESULTS AND DISCUSSIONS

6.1 Variation of Tensile Force Developed In Geogrid Reinforcement at Different Locations

Gnanendran and Selvadurai (2001) installed 12 pair of strain gauges to capture the variation of local strain developed in geogrid reinforcement at different locations. Those strain gauges are calibrated before and after the physical model test to obtain the tensile force developed at the corresponding locations. The experimental results indicate that the tensile force across the geogrid varies from zero at the ends and increases up to a maximum value at a point close to the foundation. In order to capture the variation of tensile force developed in geogrid reinforcement at different locations through numerical analysis, different points at regular interval along the centre line of the geogrid sheet was identified by their component identification (CID) number. Then the stresses developed per meter length at those selected points while applying footing load are recorded by “history” command. Finally from the recorded data file, the geogrid force contour as a percentage of ultimate footing load were plotted at three different loading stage (e.g. when footing load is 40% and 100% of ultimate load) and compared with the experimental results. Both the analytical and experimental plots matched well which proof the numerical predictability of the created reinforced model slope as shown in figure 4 and 5. Figure 6 also shows the contour of stress developed per unit length of geogrid where the maximum stress occurs just below the footing.

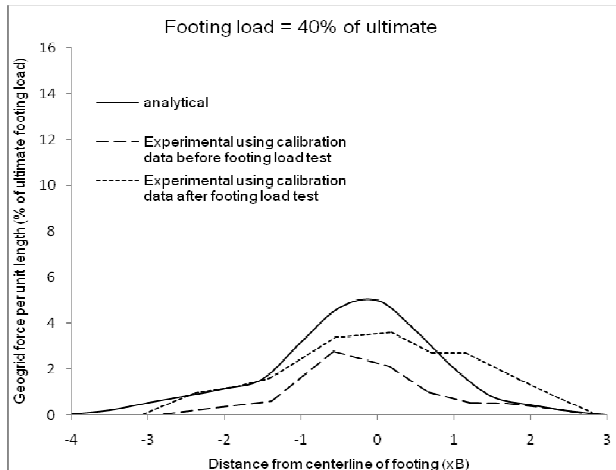


Figure 4: Variation of the tensile force across the geogrid reinforcement when footing load was 40% of ultimate

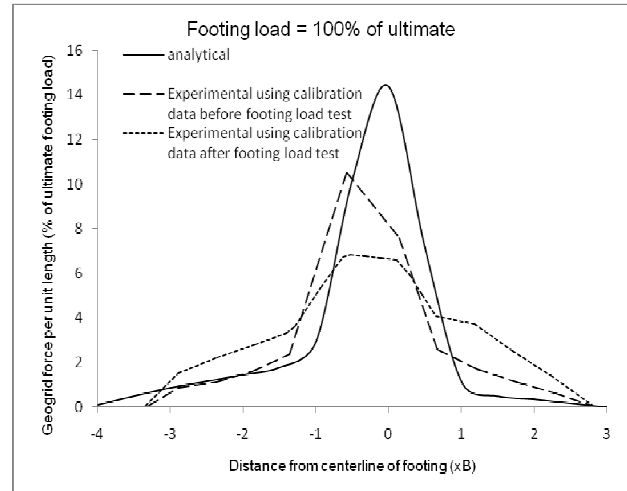


Figure 5: Variation of the tensile force across the geogrid reinforcement when footing load was 100% of ultimate

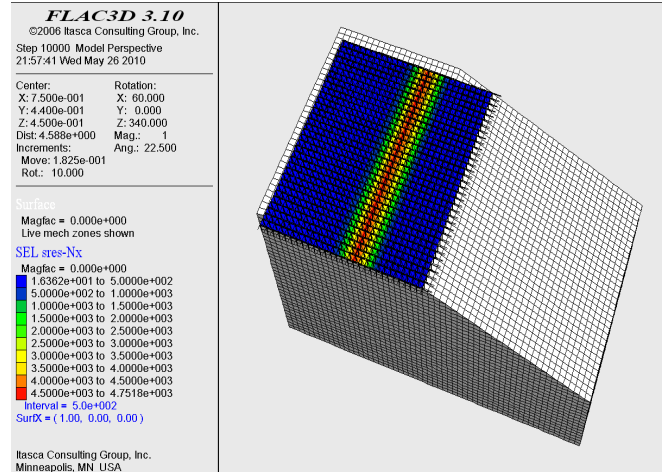


Figure 6: Contour of stress developed per unit length of geogrid

6.2 Variation of Maximum Tensile Force Developed in Geogrid Reinforcement With Applied Footing Load

From the plot of tensile force distribution over geogrid reinforcement, both the experimental and numerical result shows that the maximum geogrid tensile force occurs at a location close to the centre line of footing base. Thus a geogrid element just below the footing is selected and the variation of tensile force developed in geogrid at that element with applied footing load was monitored. Then the geogrid tensile force versus applied footing pressure were plotted and compared with the experimental plot. Both the analytical and experimental plot as shown in figure 7 agreed well and indicates that the applied foundation pressure and the maximum tensile force developed in the layer of geogrid reinforcement are not linearly related.

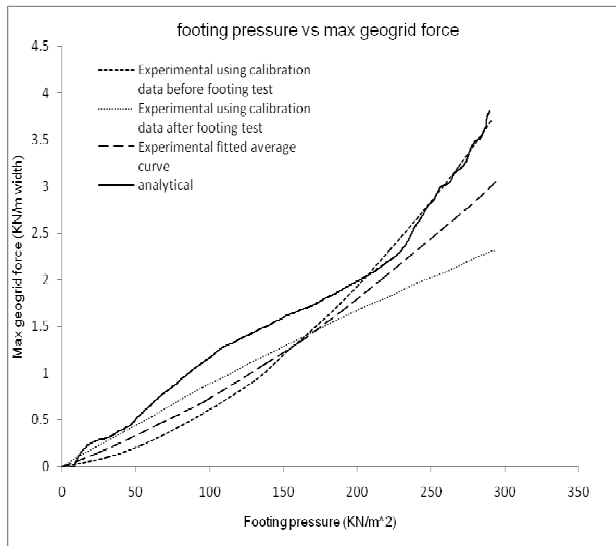


Figure 7: Variation of the maximum tensile force in the geogrid reinforcement versus applied footing pressure

7 CONCLUSIONS

The geogrid reinforcement provides stability to the slope fill structure mainly due to their tensile stiffness rather than bending stiffness. Thus the accurate estimation of tensile force developed in geogrid at different location while subjected to footing load is very important for the design of reinforced slope fill structure. But in physical model study, it is very difficult to determine the tensile force developed in geogrid by using calibrated strain gauges as described by Gnanendran and Selvadurai (2001). The use of numerical analysis software FLAC3D for computing the tensile force developed in geogrid while used as reinforcement in a sloped fill and subjected to footing load is a very good option. After several attempts taken by researches using different numerical analysis software, they fail to get a satisfactory prediction for the stabilizing force provided by geogrid. In this paper both the predicted load–settlement plot of footing and tensile force developed in geogrid matched well with the published experimental plot. Thus it can be concluded that the developed 3D numerical model has a very good capability to predict the behaviour of footing on reinforced sloped fill as well as stabilizing force developed in the geogrid layer and can be used for predicting real field problem.

ACKNOWLEDGEMENT

The author would like to acknowledge the contribution of University of New South Wales at Australian Defence Force Academy (UNSW@ADFA) for providing scholarship.

REFERENCES

- Alamshahi, S., Hataf, N., 2009. Bearing capacity of strip footings on sand slopes reinforced with geogrid and grid-anchor. *Geotextiles and Geomembranes* 27, 217-226.
- Bathurst, R.J., Blatz, J.A., Burger, M.H., 2003. Performance of instrumented large-scale unreinforced and reinforced embankments loaded by a strip footing to failure. *Can Geotech J* 40, 1067 - 1083.
- Duncan, J.M., Chang, C.Y., 1970. Nonlinear analysis of stress and strain in soils. *Soil Mechanics and Foundation Engineering Division, ASCE* 96, 1629 - 1653.
- Gnanendran, C.T., 2001. Prediction of the behaviour of a geogrid reinforced sloped fill under footing load. In: *Landmarks in Earth Reinforcement*, A.A.B.P. (Ed.), Proceedings of the International Symposium on Earth Reinforcement – IS Kyushu 2001 Fukuoka, Japan., pp. 559-564.
- Gnanendran, C.T., Selvadurai, A.P.S., 2001. Strain measurement and interpretation of stabilising force in geogrid reinforcement. *Geotextiles and Geomembranes* 19, 177-194.
- Guido, V.A., Chang, D.K., Sweeney, M.A., 1986. Comparison of geogrid and geotextile reinforced earth slabs. *Can Geotech J* 23, 435-440.
- Itasca Consulting Group, I., 2006. *Fast Lagrangian Analysis of Continua in 3 Dimensions (FLAC3D)*. Itasca Consulting Group, Inc., Minneapolis, Minnesota 55401 USA.
- Jewell, R.A., Milligan, G.W.E., Sarsby, R.W., Dubois, D., 1984. Interaction between soil and geogrids. *Proc. of the Symp. on Polymer Grid Reinforcement in Civil Engng.*, Thomas Telford Limited, London, pp. 18 - 29.
- Selvadurai, A.P.S., Gnanendran, C.T., 1989. An experimental study of a footing located on a sloped fill: influence of a soil reinforcement layer. *Can Geotech J* 26, 467-473.
- Thanapalasingam, J., Gnanendran, C.T., 2008. Predicting the Performance of Foundations Near Reinforced Sloped Fills. *The 12th International Conference of International Association for Computer Methods and Advances in Geomechanics (IACMAG)*, Goa, India, pp. 3727 - 3734.
- Yoo, C., 2001. Laboratory investigation of bearing capacity behavior of strip footing on geogrid-reinforced sand slope. *Geotextiles and Geomembranes* 19, 279-298.